# Modeling Quasi-elastic Form Factors for Electron and Neutrino Scattering

H. Budd[a], A. Bodek[a] and J. Arrington[b]

[a]Department of Physics and Astronomy, University of Rochester, Rochester, New York 14618, USA

[b]Argonne National Laboratory, Argonne, Illinois 60439, USA

We calculate the total and differential quasielastic cross sections for neutrino and antineutrino scattering on nucleons using up to date fits to the nucleon elastic electromagnetic form factors $G_E^p$, $G_E^n$, $G_M^p$, $G_M^n$, and weak and pseudoscalar form factors. We find that using the updated non-zero value of $G_E^n$ has a significant effect on both the total and differential neutrino and antineutrino quasielastic cross sections. Previous extractions of the weak axial form factor from neutrino scattering data are sensitive to the assumptions that were used for the vector form factors. We perform a re-analysis of previous neutrino data using updated form factors and obtain updated value of the axial vector mass. (Presented by Howard Budd at NuInt02, Dec. 2002, Irvine, CA, USA [1])

## 1. INTRODUCTION

Experimental evidence for oscillations among the three neutrino generations has been recently reported [2]. Since quasielastic (QE) scattering forms an important component of neutrino scattering at low energies, we have undertaken to investigate QE neutrino scattering using the latest information on nucleon form factors.

Recent experiments at SLAC and Jefferson Lab (JLab) have given precise measurements of the vector electromagnetic form factors for the proton and neutron. These form factors can be related to the form factors for QE neutrino scattering by conserved vector current hypothesis, CVC. These more recent form factors can be used to give better predictions for QE neutrino scattering.

## 2. EQUATIONS FOR QE SCATTERING

The hadronic current for QE neutrino scattering is given by [3]

$$< p(p_2)|J_\lambda^+|n(p_1) >= \overline{u}(p_2)\left[\gamma_\lambda F_V^1(q^2) + \frac{i\sigma_{\lambda\nu}q^\nu\xi F_V^2(q^2)}{2M} + \gamma_\lambda\gamma_5 F_A(q^2) + \frac{q_\lambda\gamma_5 F_P(q^2)}{M}\right]u(p_1),$$

where $q = k_\nu - k_\mu$, $\xi = (\mu_p - 1) - \mu_n$, and $M = (m_p + m_n)/2$. Here, $\mu_p$ and $\mu_n$ are the proton and neutron magnetic moments. We assume that there are no second class currents, so the scalar form factor $F_V^3$ and the tensor form factor $F_A^3$ need not be included. Using the above current, the cross section is

$$\frac{d\sigma^{\nu,\,\overline{\nu}}}{dq^2} = \frac{M^2G_F^2cos^2\theta_c}{8\pi E_\nu^2}\times \left[A(q^2) \mp \frac{(s-u)B(q^2)}{M^2} + \frac{C(q^2)(s-u)^2}{M^4}\right],$$

where

$$A(q^2) = \frac{m^2-q^2}{4M^2}\left[\left(4-\frac{q^2}{M^2}\right)|F_A|^2 - \left(4+\frac{q^2}{M^2}\right)|F_V^1|^2 - \frac{q^2}{M^2}|\xi F_V^2|^2\left(1+\frac{q^2}{4M^2}\right) - \frac{4q^2ReF_V^{1*}\xi F_V^2}{M^2}\right],$$

$$B(q^2) = -\frac{q^2}{M^2}ReF_A^*(F_V^1 + \xi F_V^2),$$

$$C(q^2) = \frac{1}{4}\left(|F_A|^2 + |F_V^1|^2 - \frac{q^2}{M^2}\left|\frac{\xi F_V^2}{2}\right|^2\right).$$

Although we have have not shown terms of order $(m_l/M)^2$, and terms including $F_P(q^2)$ (which is multiplied by $(m_l/M)^2$), these terms are included in our calculations [3].) The form factors $F_V^1(q^2)$

| | |
|---|---|
| $g_A$ | -1.267 |
| $G_F$ | $1.1803\times10^{-5}$ GeV$^{-2}$ |
| $\cos\theta_c$ | 0.9740 |
| $\mu_p$ | 2.793 $\mu_N$ |
| $\mu_n$ | -1.913 $\mu_N$ |
| $\xi$ | 3.706 $\mu_N$ |
| $M_V^2$ | 0.71 GeV$^2$ |

Table 1
The most recent values of the parameters used in our calculations (Unless stated otherwise).

and $\xi F_V^2(q^2)$ are given by:

$$F_V^1(q^2) = \frac{G_E^V(q^2) - \frac{q^2}{4M^2}G_M^V(q^2)}{1-\frac{q^2}{4M^2}},$$

$$\xi F_V^2(q^2) = \frac{G_M^V(q^2) - G_E^V(q^2)}{1-\frac{q^2}{4M^2}}.$$

We use the CVC to determine $G_E^V(q^2)$ and $G_M^V(q^2)$ from the electron scattering form factors $G_E^p(q^2)$, $G_E^n(q^2)$, $G_M^p(q^2)$, and $G_M^n(q^2)$:

$$G_E^V(q^2) = G_E^p(q^2) - G_E^n(q^2),$$
$$G_M^V(q^2) = G_M^p(q^2) - G_M^n(q^2).$$

Previously, many neutrino experiment have assumed that the vector form factors are described by the dipole approximation.

$$G_D(q^2) = \frac{1}{\left(1-\frac{q^2}{M_V^2}\right)^2}, \quad M_V^2 = 0.71\ GeV^2$$

$$G_E^p = G_D(q^2), \quad G_E^n = 0,$$
$$G_M^p = \mu_p G_D(q^2), \quad G_M^n = \mu_n G_D(q^2).$$

We refer to the above combination of form factors as 'Dipole Form Factors'. It is an approximation that is improved upon in this paper. We will refer to our updated form factors as 'BBA-2003 Form Factors' (Budd, Bodek, Arrington). Table 1 summarizes the most up to date values of the coupling constants and magnetic moments that we use in our calculations. Note that $G_E^p$, $G_M^p$, and $G_E^n$ are positive, while $G_M^n$ and the axial form factor $F_A$ are negative.

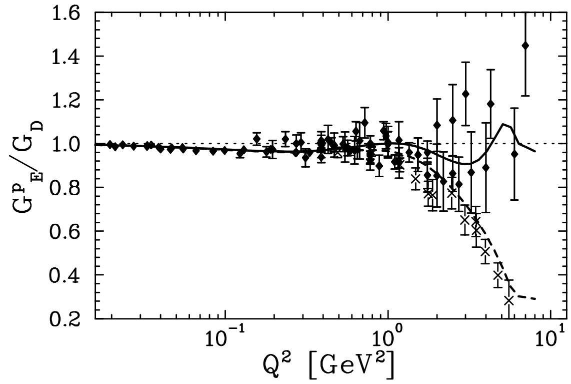


Figure 1. Our fits to $G_E^p/G_D$, using cross section data only (solid), and with both the cross section and polarization transfer data (dashed). The diamonds are the from Rosenbluth extractions and the crosses are the Hall A polarization transfer data. Note that we fit to cross sections, rather than fitting directly to the extracted values of $G_E^p$ shown here.

The axial form factor is given by

$$F_A(q^2) = \frac{g_A}{\left(1-\frac{q^2}{M_A^2}\right)^2}.$$

This form factor needs to be extracted from QE neutrino scattering. However, at low $Q^2$, this form factor can also be extracted from pion electroproduction data.

Previous neutrino experiments used $g_A$=$-1.23$, while the best current value is $-1.267$. The world average from neutrino experiments for $M_A$ is 1.026 ± 0.020 GeV [4]. The value of $M_A$ extracted from neutrino experiments depends on both the value of $g_A$ and the values of the electromagnetic form factors which are assumed in the extraction process. Since we are updating these form factors, new values of $M_A$ are extracted from previous neutrino data using the better known values for $g_A$ and the vector form factors.

$M_A$ can also be determined from pion electroproduction, which yields a world average value of 1.069 ± 0.016 GeV [4]. This value should be reduced by 0.055 GeV when compared to $M_A$ as

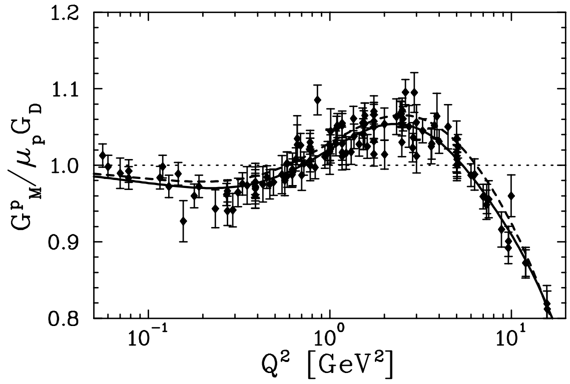


Figure 2. Our fits to $G_M^p/\mu_p G_D$. The lines and symbols have the same meaning as Figure 1.

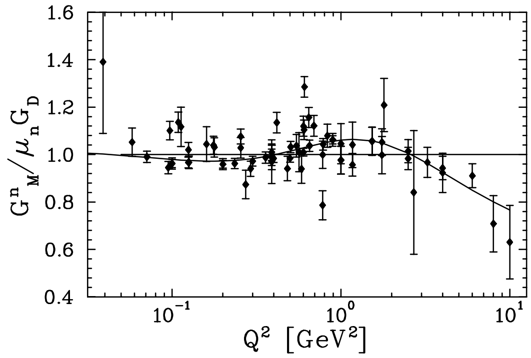


Figure 3. Our fit to $G_M^n/\mu_n G_D$. The lines and symbols have the same meaning as Figure 1.

measured in neutrino data because of additional corrections [4]. Therefore, pion electroproduction experiments predict that $M_A$ should be $1.014 \pm 0.016$ GeV in neutrino scattering.

In this communication, we show that the value of $1.026 \pm 0.02$ GeV [4] as measured from the average of all neutrino scattering should also be reduced by 0.025 GeV to account for incorrect vector form factors used in the past. This corrected value of $1.001 \pm 0.020$ GeV is in good agreement with the theoretically corrected value from pion electroproduction of $1.014 \pm 0.016$ GeV.

From PCAC, the pseudoscalar form factor $F_P$ is predicted to be

$$F_P(q^2) = \frac{2M^2 F_A(q^2)}{M_\pi^2 - q^2}.$$

In the expression for the cross section, $F_P(q^2)$ is multiplied by $(m_l/M)^2$. Therefore, in muon neutrino interactions, this effect is very small except at very low energy, below 0.2 GeV. The effect is larger, about 5%, for tau neutrino interactions.

## 3. UPDATED FORM FACTORS

We have used an updated fit to the proton electromagnetic form factors. The fit is similar to the one described in Ref. [5], but using a slightly different fitting function (described below), and including additional data to constraint the fit at low $Q^2$ values. Form factors can be determined from cross sections using the standard Rosenbluth separation technique [5], which is sensitive to radiative corrections, or from polarization measurements using the newer polarization transfer technique [6]. The polarization measurements do not directly measure the form factors, but measure the ratio $G_E/G_M$. Figures 1, 2, and 3 show the ratio of our fits divided by the dipole form, $G_D$.

Figure 4 shows our fits to $\mu_p G_E^p/G_M^p$. The fit including only cross section data is roughly flat versus $Q^2$ ($Q^2 = -q^2$), while ratio decreases with $Q^2$ in the combined fit to cross section and polarization transfer data. Although the polarization transfer measurement is believed to have smaller systematic error, especially at high $Q^2$, the origin of this disagreement is not known. If this disagreement comes from radiative corrections to the electron, in particular two-photon exchange terms, then the polarization transfer extraction will give the correct ratio, but the overall scale of $G_E^p$ at low $Q^2$ would be shifted down by $\approx$3%. Because the fit is constrained as $Q^2 \to 0$, there will not be an overall shift in $G_E^p$ at low $Q^2$, but there will be some uncertainty in the low $Q^2$ behavior. Current experiments at JLab aim to better understand the source of the disagreement by looking at the recoil proton in elastic electron-proton scattering, thus minimizing the sensitivity to the dominant sources of uncertainty in previous Rosenbluth separations. However, since this discrepancy is most prominent at high $Q^2$, and the fit is constrained at low $Q^2$, it has only a rel-

| | data | $a_2$ | $a_4$ | $a_6$ | $a_8$ | $a_{10}$ | $a_{12}$ |
|---|---|---|---|---|---|---|---|
| $G_E^p$ | CS + Pol | 3.253 | 1.422 | 0.08582 | 0.3318 | -0.09371 | 0.01076 |
| $G_M^p$ | CS + Pol | 3.104 | 1.428 | 0.1112 | -0.006981 | 0.0003705 | -0.7063E-05 |
| $G_M^n$ | | 3.043 | 0.8548 | 0.6806 | -0.1287 | 0.008912 | |
| $G_E^p$ | CS | 3.226 | 1.508 | -0.3773 | 0.6109 | -0.1853 | 0.01596 |
| $G_M^p$ | CS | 3.188 | 1.354 | 0.1511 | -0.01135 | 0.0005330 | -0.9005E-05 |

Table 2
The coefficients of the inverse polynomial fits for the $G_E^p$, $G_M^p$, and $G_M^n$. Fits using cross section data only, and using both cross section data and the Hall A polarization transfer data are shown separately. Note that these different polynomials replace $G_D$ in the expression for $G_E^p$, $G_M^p$, and $G_M^n$. The first three rows of the table along with the fit of $G_M^p$ Krutov *et. al.* [7] (see text) will be referred to as 'BBA-2003 Form Factors'.

atively small effect on the neutrino QE scattering cross section.

To account for the fact that deviations from the dipole form are different for each of the different form factors, we fit electron scattering data for each of the form factors to an inverse polynomial

$$G_{E,M}^N(Q^2) = \frac{G_{E,M}^N(Q^2=0)}{1 + a_2Q^2 + a_4Q^4 + a_6Q^6 + ...}.$$

Table 2 shows the parameters of our fit. We have done fits using cross section data only (for the proton) and fits using both both cross section data and polarization transfer data from JLab Hall A. For $G_E^p$, the parameters in Table 2 are used for $Q^2 < 6$ GeV$^2$. For $Q^2 > 6$ GeV$^2$, the ratio of $G_E^p/G_M^p$ is assumed to be constant:

$$G_E^p(Q^2) = G_M^p(Q^2)\frac{G_E^p(6 \text{ GeV}^2)}{G_M^p(6 \text{ GeV}^2)}$$

Since the neutron has no charge, $G_E^n$ must be zero at $q^2$=0, and previous neutrino experiments assumed $G_E^n(q^2)$=0 for all $q^2$ values. However, it is non-zero away from $q^2$=0, and its slope at $q^2$=0 is known precisely from neutron-electron scattering. At intermediate $Q^2$, recent polarization transfer data give precise values of $G_E^n(q^2)$. Our analysis uses the parameterization of Krutov *et. al.* [7]:

$$G_E^n(Q^2) = -\mu_n\frac{a\tau}{1+b\tau}G_D(Q^2), \quad \tau = \frac{Q^2}{4M^2},$$

with $a = 0.942$ and $b = 4.61$. This parameterization is very similar to that of Galster *et al.* [8], as shown in Figure 5.

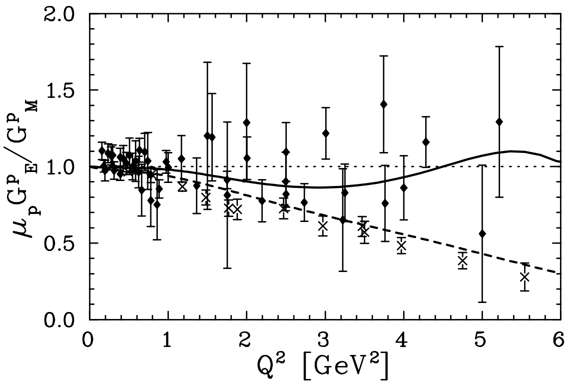


Figure 4. Ratio of $G_E^p$ to $G_M^p$ as extracted by Rosenbluth measurements and from polarization measurements. The lines and symbols have the same meaning as Figure 1.

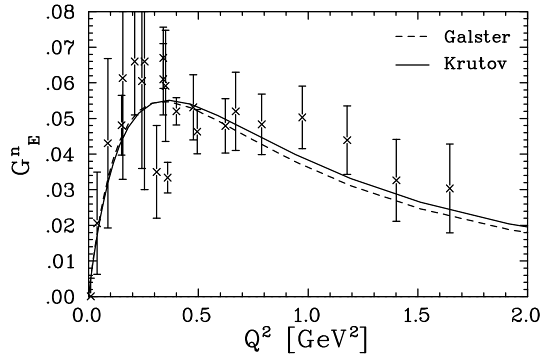


Figure 5. Data and fits to $G_E^n$. The dashed line is the Galster *et al.* fit [8], and the solid line is the Krutov*et al.* fit [7].

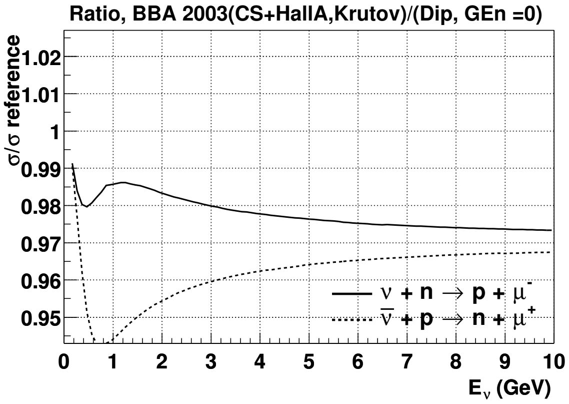


Figure 6. Ratio versus energy of predicted neutrino (antineutrino) QE cross section using BBA-2003 Form Factors to the prediction using the dipole approximation with $G_E^n$=0.

The first three rows of Table 2, along with the fit of $G_E^n$ of Krutov *et. al.* [7], will be referred to as 'BBA-2003 Form Factors'. For BBA-2003 Form Factors, both the cross section and polarization data are used in the extraction of $G_E^p$ and $G_M^p$.

## 4. CROSS SECTIONS AND FITS TO $M_A$

Figure 6 shows the ratio versus neutrino energy of the predicted neutrino (antineutrino) QE cross section using our BBA-2003 Form Factors to the prediction using the Dipole Form Factors. The same comparison was performed using the proton form factor extractions that included only the cross section data (*i.e.* excluding the polarization results). The results were nearly identical: the maximum difference between the cross sections is less then 0.3%. This is because the form factors extracted from the polarization transfer data and from the electron scattering cross section data are different only at high $Q^2$, while the neutrino cross sections are mostly sensitive to the form factors at low $Q^2$.

There is a large difference in the predicted neutrino (antineutrino) cross section between using the BBA-2003 Form Factors and using the Dipole Form Factor approximation. The difference is 3% at high energy and can become as much as

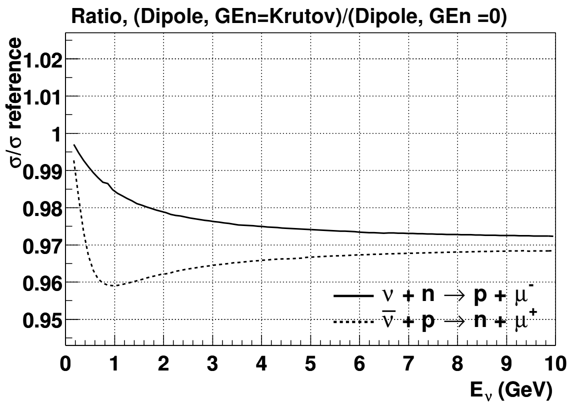


Figure 7. Ratio versus energy of the predicted neutrino (antineutrino) QE cross section using $G_E^n$ from Krutov [7] to the prediction using $G_E^n$=0. In both cases, the dipole approximation for the other form factors.

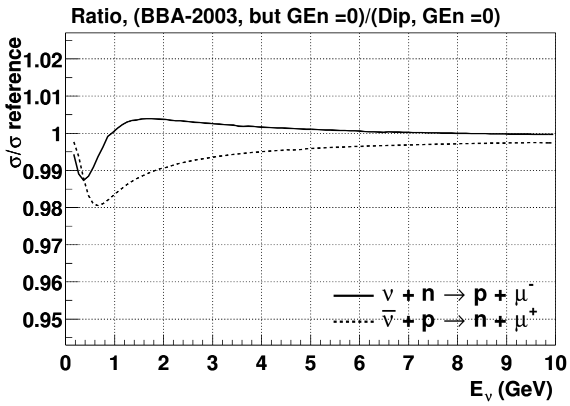


Figure 8. Ratio versus energy of predicted neutrino (antineutrino) QE cross section using our BBA-2003 Form Factor fits for $G_E^p$, $G_M^p$, and $G_N^n$ to the prediction using the dipole approximation. In both cases, we use $G_E^n$=0.

6% at 1 GeV. As seen in Figure 7, which shows the difference between $G_E^n$ = Krutov and $G_E^n$ = 0, all the difference at high energy and most of the the difference at low energy is due to $G_E^n$. At the low energy region which is of interest for neutrino oscillation experiments, both a non-zero $G_E^n$ and the deviations from the dipole form are important. This is also the case for the extraction of the axial form factor from neutrino data, since most of the neutrino differential cross section data are at low $Q^2$.

A 1% increase in either $M_A$ or $|g_A|$ increases the cross section about 1%. Replacing the old value of $g_A$=−1.23 with the more precise value of $g_A$=−1.267 increases the cross section by about 2.5%. Using the more recent value of $M_A$ of 1.02 instead of the older value of 1.032 decreases the predicted cross section about 1%. $F_P$ has almost no effect on the cross section except at very low $E_\nu$. Therefore, even a very conservative error [4] on $F_P$ of 50% has very little effect.

Previous neutrino measurements, mostly bubble chamber experiments, extracted $M_A$ using the best known assumptions at the time. Changing these assumptions changes the extracted value of $M_A$. Hence, $M_A$ needs to be updated using new form factors and up-to-date couplings. In this communication we will attempt to update the results from three previous deuterium bubble chamber experiments. These are Baker *et al.* [9], Barish *et al.* [10], Miller *et al.* [11], and Kitagaki *et al.* [12]. Barish *et al.* and Miller *et al.* are the same experiment, with the analysis of Miller *et al.* including the full data set, roughly three times the statistics included in the original analysis.

We start by calculating the shape of the $Q^2$ distribution using the same form factors and couplings as used in the original extractions (including $M_A$). The flux is extracted from the flux figures shown in the original papers, which we parameterize using a spline fit. We extract the data and curves from their publications by picking points off the plots, and fitting the points on the curves to a spline fit. These experiments did not use a pure dipole approximation, but included a correction to the dipole form as parameterized by Olsson *et al.* [14]. They use $g_A$=−1.23, $M_V$=0.84 GeV (yielding $M_V^2$=0.7056 GeV$^2$ in-

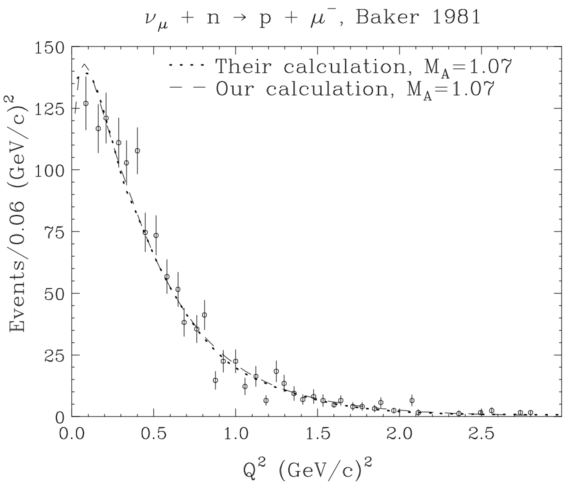


Figure 9. $Q^2$ distribution from Baker *et al.* [9]. The dotted curve is their calculation taken from their $Q^2$ distribution histogram. The dashed curve is our calculation using their assumptions.

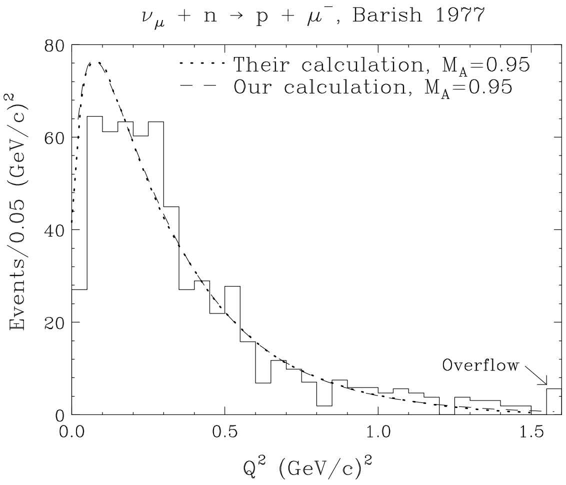


Figure 10. $Q^2$ distribution from Barish *et al.* [10]. The dotted curve is their calculation taken from their $Q^2$ distribution histogram. The dashed curve is our calculation using their assumptions.

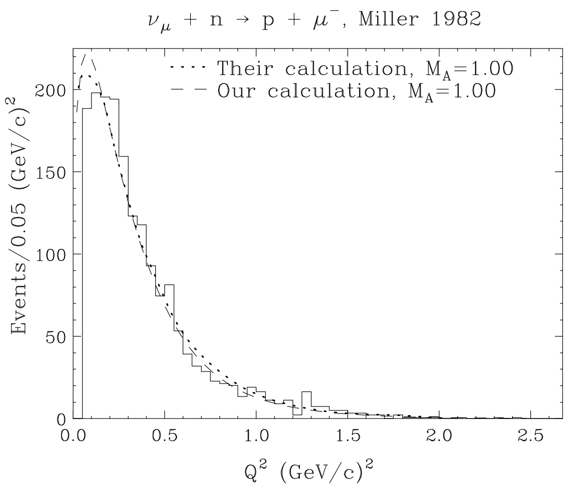


Figure 11. $Q^2$ distribution from Miller *et al.* [11]. The dotted curve is their calculation taken from their $Q^2$ distribution histogram. The dashed curve is our calculation using their assumptions.

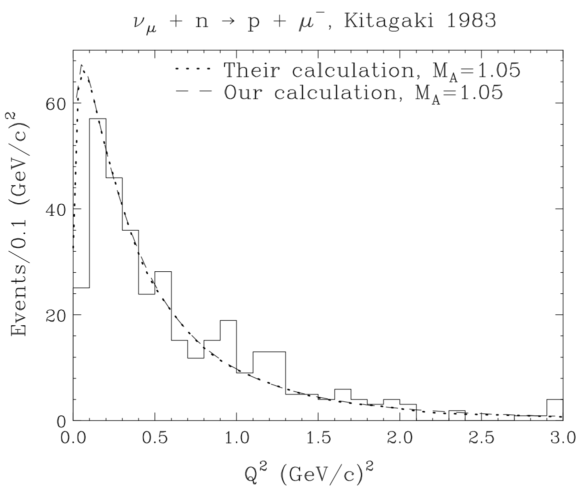


Figure 12. $Q^2$ distribution from Kitagaki *et al.* [12]. The dotted curve is their calculation taken from their $Q^2$ distribution histogram. The dashed curve is our calculation using their assumptions.

stead of $M_V^2$=0.71 GeV$^2$), and a $D_2$ Pauli-suppression correction from Singh *et al.* [15]. Our calculations and their calculations are compared in Figures 9, 10, 11, and 12. In these figures, our curves are normalized such that they match the previous curves at one point in the low $Q^2$ region, so that we can compare the $Q^2$-dependence of the spectra. The y-axis is weighted events/bin (corrected for efficiencies). We reproduce the shape ($Q^2$-dependence) of the calculations of Baker *et al.* [9], Barish *et al.* [10], and Kitagaki *et al.* [12], but not Miller *et al.* [11]. As Miller *et al.* gives an updated result of Barish *et al.*, they should be using the same calculation. Therefore, we do not understand the origin of the curve shown in Miller *et al.*

Having reproduced the calculations under the same assumptions as in the original extractions, we perform our own extraction of $M_A$, using our calculation of the cross sections, but using the same input ($g_A$ and form factors) as assumed in the original extractions. Due to inefficiencies in reconstruction for very low $Q^2$ events, they do not use the first bin for fitting. Hence, we do not use the first bin for fitting or normalization either. We perform a binned maximum likelihood using a formula from the Particle Data Group [16]. The experiments performed an unbinned likelihood fit, which we cannot reproduce since we do not have the individual events. Table 3 gives the results of these fits. Using the same assumptions, we reproduce the fitted value of $M_A$ from Baker *et al.*, while disagreeing somewhat with the values from Barish *et al.*, Miller *et al.*, and Kitagaki *et al.* The difference may come from the fact that we are forced to use a binned likelihood fit, rather than being able to reproduce their unbinned fit.

Figures 13 and 14 show the difference between using their value of $M_A$ and our value of $M_A$ for Kitagaki *et al.* and Barish *et al.* The plot for Kitagaki *et al.* appears to show that our value of $M_A$=1.19 GeV is a better fit than their value of $M_A$. For Barish *et al.* its not clear which is a better fit. As previously stated, our $Q^2$ distribution is slightly different than that of Miller *et al.* for the same $M_A$. Figure 15 shows their calculation for their best fit $M_A$ versus our calculation using our best fit $M_A$. The two shapes agree very

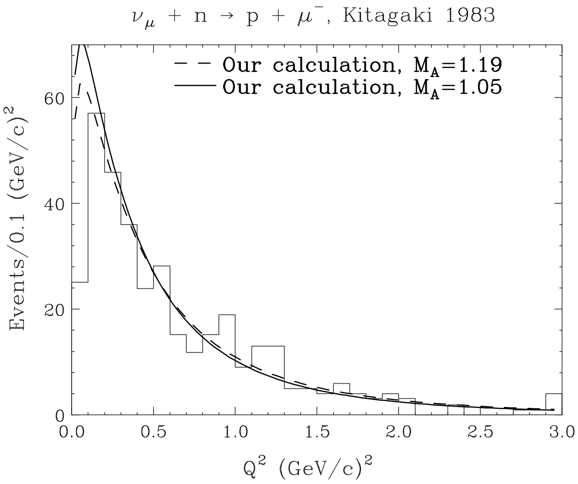


Figure 13. $Q^2$ distribution from Kitagaki *et al.* [12]. The dash curve is our calculation using our fit value of $M_A$=1.19 GeV. The solid curve is our calculation using their fit value of $M_A$=1.05 GeV.

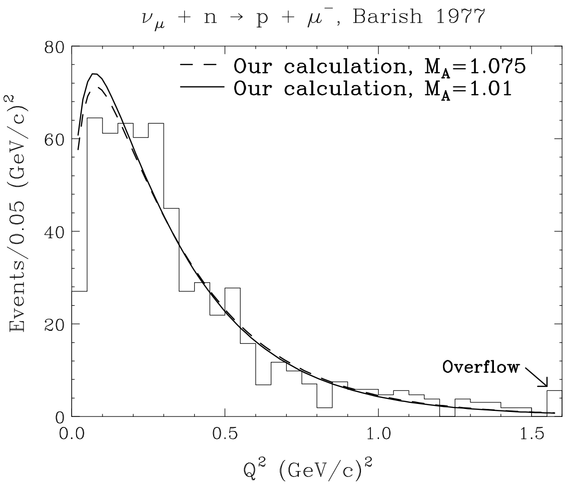


Figure 14. $Q^2$ distribution from Barish *et al.* [10]. The dash curve is our calculation using our fit value of $M_A$=1.075 GeV. The solid curve is our calculation using their fit value of $M_A$=1.01 GeV.

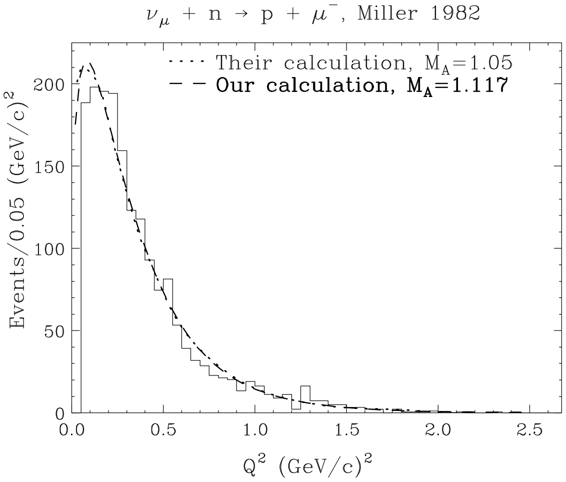


Figure 15. $Q^2$ distribution from Miller *et al.* [11]. The dotted curve is their calculation using their fit value of $M_A$=1.05 GeV. The dash curve is our calculation using our fit value of $M_A$=1.117 GeV.

well. Hence, we are able to reproduce the best fit shape of Miller *et al.* fit, but not with their value of $M_A$.

Finally, we extract $M_A$ for each of these experiments using our calculations with the updated BBA-2003 Form Factors and $g_A$ value. Comparing this to our extraction with their input parameters, we obtain change in $M_A$ due to using updated values for $g_A$ and the form factors. Because we sometimes obtain slightly different values of $M_A$, even with the same input parameters, we take the difference between our extraction with old and new form factors as the modification that should be applied to the previous extractions, which were able to do a more detailed comparison to their data. Table 3 gives the results of these fits, which indicate that we should shift the value of $M_A$ determined from deuterium by $-0.025$ GeV from the value quoted by these experiments. We also show that a shift in $M_A$ of $-0.050$ GeV is required in going from the Dipole Form Factors to BBA-2003 Form Factors, keeping $g_A$ constant. If only cross section data were used for the form factor fits (Table 1, rows 4 and 5), the value of $M_A$ would go up by 0.002 GeV, a

| | $M_A$ (published) | updated $M_A$ old params. | updated $M_A$ new params. | $\Delta M_A$ new–old | $\Delta M_A$ BBA-2003–Dipole |
|---|---|---|---|---|---|
| Baker 1981 [9] | 1.07 ± 0.06 | 1.079 ± 0.056 | 1.055 ± 0.055 | −0.024 | −0.049 |
| Barish 1977 [10] | 1.01 ± 0.09 | 1.075 ± 0.10 | 1.049 ± 0.099 | −0.026 | −0.046 |
| Miller 1982 [11] | 1.05 ± 0.05 | 1.117 ± 0.055 | 1.090 ± 0.055 | −0.027 | −0.046 |
| Kitagaki 1983 [12] | $1.05^{+0.12}_{-0.16}$ | $1.194^{+0.10}_{-0.11}$ | $1.175^{+0.10}_{-0.11}$ | −0.019 | −0.050 |

Table 3
Published and updated extractions of $M_A$ (GeV) from deuterium experiments. The first value of $M_A$ is the values extracted in the original publications. For Barish and Miller, we give their 'shape fit' value, since this value most closely reflects how we can calculate their $M_A$. The second value of $M_A$ is from the analysis presented here, using the same input parameters (form factors and $g_A$) as in the publications, while the third uses the updated parameters from tables 2 and 1. The last two columns show the change in $M_A$ between the new and old input parameters, and the change when comparing the BBA-2003 and Dipole Form Factors (with $g_A$ fixed).

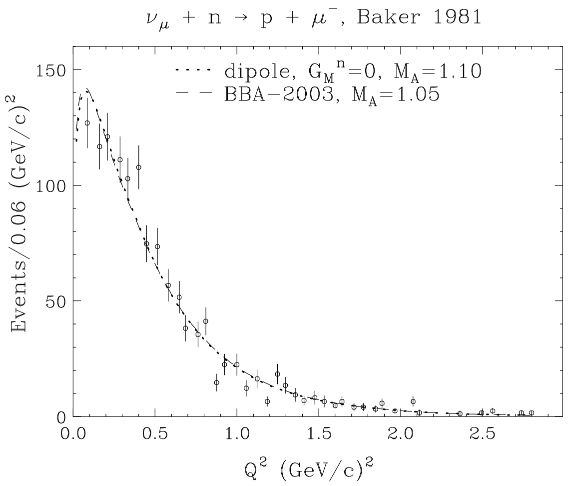


Figure 16. A comparison of the $Q^2$ distribution using 2 different sets of form factors. The data are from Baker *et al.* [9]. The dotted curve uses Dipole Form Factors with $M_A$=1.10 GeV. The dashed curve uses BBA-2003 Form Factors with $M_A$=1.05 GeV.

small effect.

Figure 16 shows the $Q^2$ distribution for Dipole Form Factors and $M_A$=1.10 GeV with the distribution for BBA-2003 Form Factors and $M_A$=1.050 GeV. When we modify the electromagnetic form factors, the modification in $M_A$ not only reproduces the original yield, it also reproduces the $Q^2$ distribution. Because there is no modification of the $Q^2$ dependence when strength is shifted between the electromagnetic and axial form factors, we conclude that the use of Dipole Form Factors will lead to an error in $M_A$ of 0.050 GeV, independent of the details of the experiment.

Figures 17 and 18 show the QE cross section for $\nu$ and $\overline{\nu}$ using our most up to date assumptions. The normalization uncertainty in the data is approximately 10%. We have used BBA-2003 Form Factors, and have scaled down $M_A$ from the old best fit of $M_A$=1.026 ± 0.021 GeV to $M_A$=1.00 GeV (which would have been obtained with the best vector form factors known today). The solid curve uses no nuclear correction, while the dotted curve [24] uses a NUANCE [26] calculation of a Smith and Moniz [25] based Fermi gas model for carbon. This nuclear model includes Pauli blocking and Fermi motion, but not final state interactions. The Fermi gas model was run with a 25 MeV binding energy and 220 MeV Fermi momentum. The updated form factors improve the agreement with neutrino QE cross section data and give a reasonable description of the cross sections from deuterium. However, the data from heavy targets, including all of the antineutrino data, are systematically below the calculation, even with the Fermi gas nuclear corrections. The only experiment on heavy nuclei which agrees with the calculation is SKAT [18] with neutrinos. The Fermi gas nuclear correction may not be sufficient. Tsushima *et al.* [27]

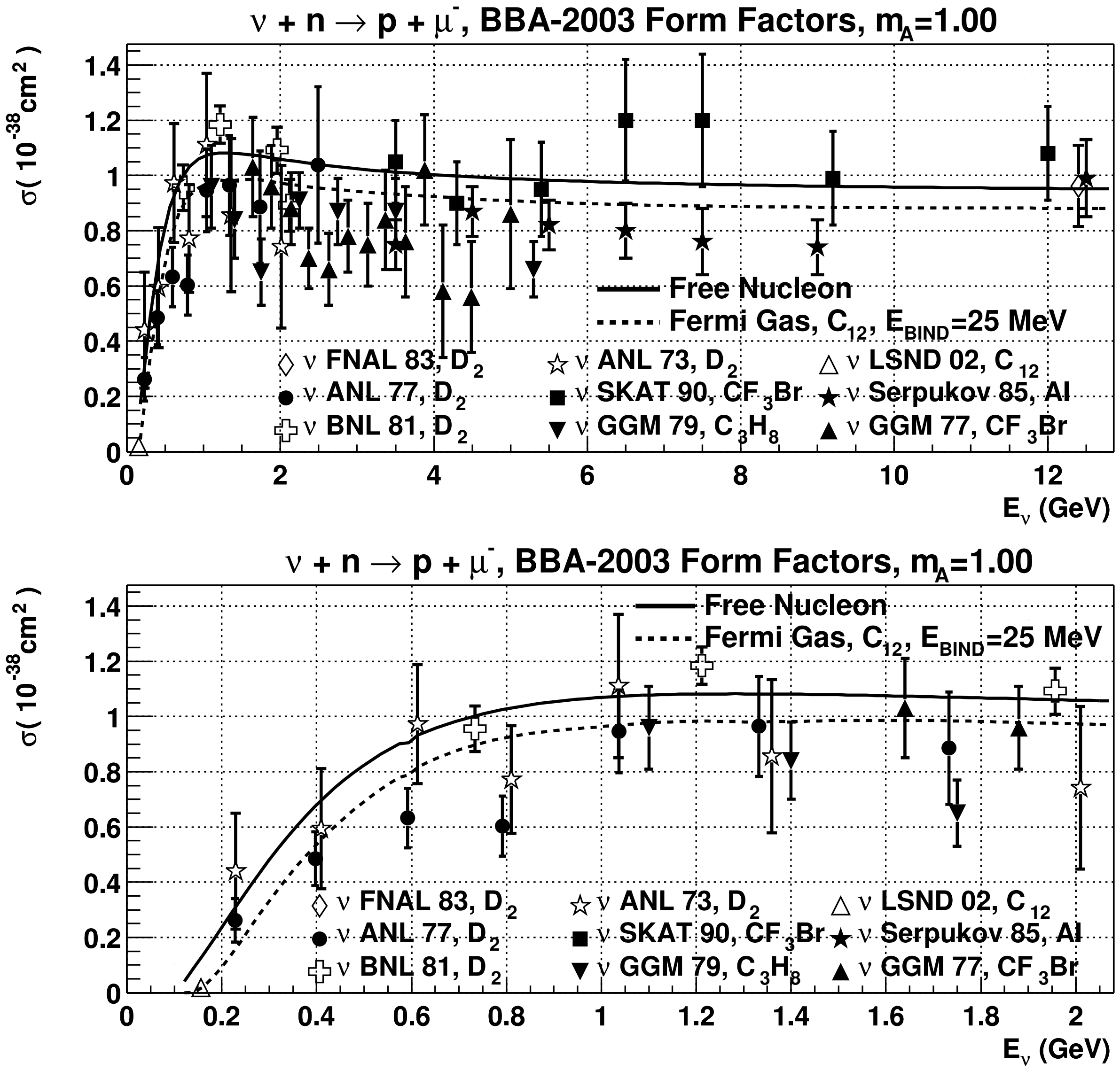


Figure 17. The QE neutrino cross section along with data from various experiments. The calculation uses $M_A$=1.00 GeV, $g_A$=−1.267, $M_V^2$=0.71 GeV$^2$ and BBA-2003 Form Factors. The solid curve uses no nuclear correction, while the dotted curve [24] uses a Fermi gas model for carbon with a 25 MeV binding energy and 220 Fermi momentum. The lower plot is identical to the upper plot with the $E_\nu$ axis limit changed to 2 GeV. The data shown are from FNAL 1983 [12], ANL 1977 [10], BNL 1981 [9], ANL 1973 [17], SKAT 1990 [18], GGM 1979 [19], LSND 2002 [20], Serpukov 1985 [21], and GGM 1977 [22].

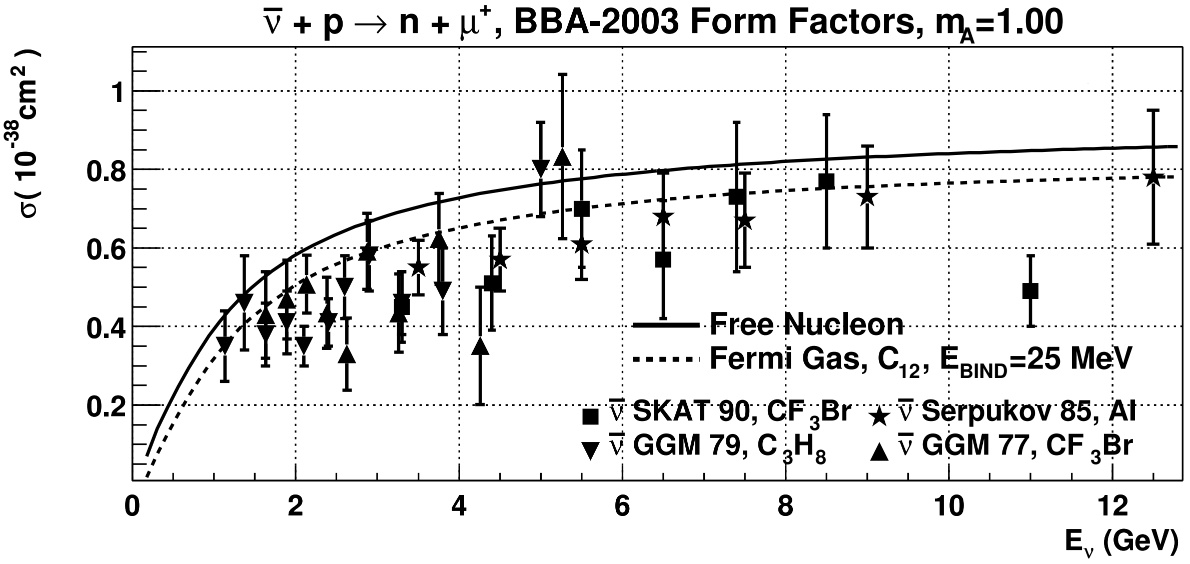


Figure 18. The QE antineutrino cross section along with data from various experiments. The calculation uses $M_A$=1.00 GeV, $g_A$=−1.267, $M_V^2$=0.71 GeV$^2$ and BBA-2003 Form Factors. The solid curve uses no nuclear correction, while the dotted curve [24] uses a Fermi gas model for carbon with a 25 MeV binding energy and 220 MeV Fermi momentum. The data shown are from SKAT 1990 [18], GGM 1979 [23], Serpukov 1985 [21], and GGM 1977 [22].

studied the effect of nuclear binding on the nucleon form factors. They stated that modifications in bound nucleon form factors reduce the cross section relative to free nucleon form factors by 8%. We plan to study the nuclear corrections, adopting models which have been used in precision electron scattering measurements from nuclei at SLAC and JLab. In addition, we will be updating the extraction of $M_A$ from other experiments, using the updated versions of the input parameters and electromagnetic form factors.

Both the overall cross section and the $Q^2$-dependence depend on the form factors chosen. However, even for input form factors that yield identical $Q^2$-dependences, the cross section can differ significantly. Figure 19 compares the cross section for two sets of form factors with identical $Q^2$ distribution (shown in Fig. 16). The figure shows that a cross section error as large as 7.5% can occur from using this combination of incorrect form factors, even though they match the '$Q^2$ shape' as well as the correct form factors

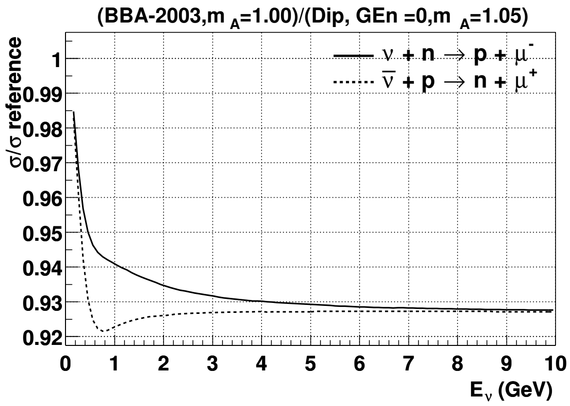


Figure 19. Ratio of cross section versus energy using BBA-2003 Form Factors with $M_A$=1.00 GeV versus Dipole Form Factors with $M_A$=1.05 GeV.

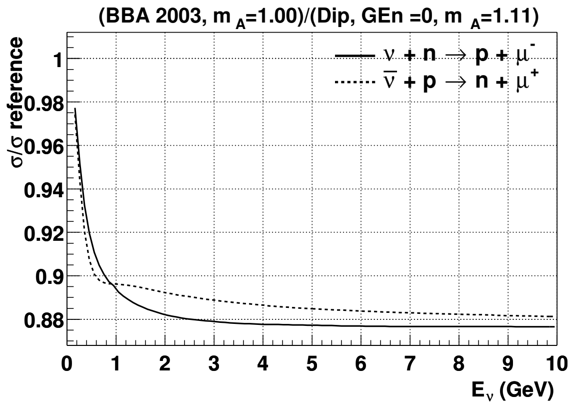


Figure 20. Ratio of cross section versus energy using BBA-2003 Form Factors with $M_A$=1.00 GeV versus Dipole Form Factors with $M_A$=1.11 GeV.

do. The effects can be even larger than in this example, especially if the $Q^2$-dependence is not required to be identical. As shown by Y. Itow's at NUINT02 talk on the results from K2K [1], the initial K2K analysis (on a water target) assumed Dipole Form Factors. They obtained a value of $M_A$=1.11 GeV and saw a low $Q^2$ suppression with respect to the predicted distribution with Dipole Form Factors and $M_A = 1.023$. Figure 20 shows the ratio vs. energy of cross sections predicted using BBA-2003 Form Factors with $M_A$=1.00 GeV to the prediction with Dipole Form Factors with $M_A$=1.11 GeV. The figure shows differences as large as 12%. This will clearly be important for future neutrino experiments at Fermilab and elsewhere: Even if the form factors which are used in the model are adjusted to describe the $Q^2$ distribution measured in a near detector neutrino experiment, one would be predicting an incorrect energy dependence of the QE cross section. Therefore, using the correct combination of form factors is important for determining the neutrino cross section and its energy dependence. An accurate measurement of QE scattering cross sections requires an accurate measurement of both the normalized cross section versus energy as well as the shape of the $Q^2$ distribution.

## 5. CONCLUSION

We have made an updated extraction of nucleon electromagnetic form factors electron scattering, and have shown these have as much as a 6% effect for neutrino-nucleon QE scattering when compared with the standard dipole approximation. Inclusion of the new form factors yields to a reduction in the value of $M_A$ extracted from neutrino scattering of 0.025 GeV. The agreement between the calculated neutrino and antineutrino free nucleon cross section and data is improved using the updated form factors, but is not spectacular, especially for data taken on heavy targets. We have shown that for a fixed $Q^2$ dependence, the neutrino cross section and its energy dependence can be affected by more than 10% if the input shapes of the electromagnetic form factors used are not correct. Hence, a complete understanding of QE scattering scattering requires an accurate measurement of both the normalized cross section versus energy as well as the shape of the $Q^2$ distribution. In addition, nuclear effects such as Pauli blocking and modification of nucleon form factors in bound nuclei need to be included. These effects are currently under investigation. For example, the simple Fermi gas model can be modified to include a high momentum tail [28] or more sophisticated spectral functions.

## 6. ACKNOWLEDGMENTS

This work is supported in part by the U. S. Department of Energy, Nuclear Physics Division, under contract W-31-109-ENG-38 (Argonne) and High Energy Physics Division under grant DE-FG02-91ER40685 (Rochester).

## REFERENCES

1. `http://www.ps.uci.edu/~nuint/`
2. Y. Fukada *et al.*, Phys. Rev. Lett. 81 (1998) 1562.
3. C.H. Llewellyn Smith, Phys. Rep. 3C (1972).
4. V. Bernard, L. Elouadrhiri, U.G. Meissner, J.Phys.G28 (2002), hep-ph[0107088].
5. J. Arrington, nucl-ex[0305009].
6. M. K. Jones *et al.*, Phys. Rev. Lett, 84, (2000)

1398 ; O. Gayou *et al.*, Phys. Rev. Lett, 88 (2002) 092301.
7. A.F. Krutov, V.E. Troitsky, Eur. Phys. J. A16 (2003) 285, hep-ph[0202183].
8. S. Glaster *et al.*, Nucl. Phys. B32 (1971) 221.
9. N.J. Baker *et al.*, Phys. Rev. D23 (1981) 2499.
10. S.J. Barish *et al.*, Phys. Rev. D16 (1977) 3103.
11. K.L. Miller *et al.*, Phys. Rev. D26 (1982) 537.
12. T. Kitagaki *et al.*, Phys. Rev. D26 (1983) 436.
13. T. Kitagaki *et al.*, Phys. Rev. Lett. 49 (1982) 98.
14. M.G. Olsson, E.T. Osyporeski and E.H. Monsay, Phys. Rev. D17 (1978) 2938.
15. S.K. Singh, Nucl. Phys. B36 (1972) 419.
16. Particle Data Group, Eur. Phys. J C15 (2000) 196.
17. W.A. Mann *et al.*, Phys. Rev. Lett. 31 (1973) 844.
18. J. Brunner *et al.*, Z. Phys. C45 (1990) 551.
19. M. Pohl *et al.*, Lett. Nuovo Cimento 26 (1979) 332.
20. L.B. Auerbach *et al.*, Phys. Rev. C66 (2002) 015501.
21. S.V. Belikov *et al.*, Z. Phys. A320 (1985) 625.
22. S. Bonetti *et al.*, Nuovo Cimento 38 (1977) 260.
23. N. Armenise *et al.*, Nucl. Phys. B152 (1979) 365.
24. G. Zeller, private communication.
25. R.A. Smith and E.J. Moniz, Nucl. Phys. B43 (1972) 605.
26. D. Casper, Nucl. Phys. Proc. Suppl. 112 (2002) 161.
27. K. Tsushima, Hungchong Kim, K. Saito, nucl-th[0307013].
28. A. Bodek and J. L. Ritchie, Phys. Rev. D23 (1981) 1070; ibid Phys. Rev. D24 (1981) 1400.